[14]C DATING OF FIRE-DAMAGED MORTARS FROM MEDIEVAL FINLAND

Alf Lindroos[1,2] • Lior Regev[3] • Markku Oinonen[4] • Åsa Ringbom[1] • Jan Heinemeier[5]

ABSTRACT. This study focuses on radiocarbon dating of mortars that have withstood city fires and display visible fire damage effects. Some fire-damaged and undamaged original Medieval mortars from the same site have also been tested. The mortars were heated at different temperatures and then analyzed using the same preparation procedures as in ^{14}C dating of mortars to see what kind of changes the heating would introduce to the mineralogy, chemistry, and the carbon and oxygen isotope ratios. We found that decarbonation during heating starts at ~600 °C and recarbonation starts as soon as the temperature drops. Already after a few days, most of the lost CO_2 has been replaced with atmospheric CO_2. The renewed carbonates are readily soluble in the acid hydrolysis process and their carbon and oxygen isotopes have a light signature. Fire-damaged historical mortars display the same features. If a long time has elapsed between hardening of the original mortar and the fire, the new carbonates have ^{14}C concentrations that point to the fire event rather than to the building event. In several cases, the fire-damaged mortars have an easily soluble carbonate fraction with a ^{14}C age that could be related to a major fire event, but still most of the soluble carbonate yields a ^{14}C age that seems like a reasonable age for the original construction.

INTRODUCTION

The introduction of accelerator mass spectrometry (AMS) into radiocarbon mortar dating (Tubbs and Kinder 1990; Van Strydonck et al. 1992) has made it possible to study the ^{14}C contribution of different carbonate components in mortar in detail and to monitor their dissolution behavior in acid hydrolysis (Heinemeier et al. 1997; Lindroos et al. 2007). The contamination capacity of aggregate limestone and unburned limestone residues from the lime burning process are thus fairly well known. As a result, ^{14}C dating has been used more frequently and an increasing number of laboratories are now involved in developing the method (e.g. Nawrocka et al. 2009; Pesce et al. 2009; Heinemeier et al. 2010; Hodgins et al. 2011; Hajdas et al., these proceedings). There are, however, still some problems to consider. One encountered frequently is fire-damaged mortars. Medieval cities in northern Europe were vulnerable to city fires caused by accident, lightning, war, and plundering. Many of the buildings that we have tried to date have burnt both fiercely and repeatedly. The preservation potential of mortared stone constructions is, however, relatively good and they may be the only preserved remnants after devastating city fires. At the sampling site, it may be obvious that the mortar has suffered damage from the fire. The whole wall is often black from soot, all that is left from wooden beams are the charred stumps, the masonry stones have fractured so that the outer surface has fallen off in an onion-skin manner, and the mortar has fallen off or falls off when poked with the chisel. This study investigates the ^{14}C inventory of the carbonate residues after fires.

Some ^{14}C profiles indicate that it seems possible to read the construction age from a ^{14}C profile of a damaged mortar if several successive CO_2 fractions yield similar ^{14}C ages and they represent a major part of the carbon inventory (Figure 1; Ringbom et al. 2005; Heinemeier et al. 2010). Note that a profile in the sense we use it here is only a smoothed line between the data points, not a modeled trend line as presented in Lindroos et al. (2007).

This study presents other ^{14}C profiles from stepwise hydrolysis of mortars that have visible fire damage from historically documented fires. Also, some preliminary experiments have been conducted by heating both fire-damaged samples and seemingly undamaged samples up to 700 °C and

[1]Åbo Akademi University, Finland.
[2]Corresponding author. Email: alindroo@abo.fi.
[3]Kimmel Center, Weizmann Institute of Science, Rehovot, Israel.
[4]Finnish Museum of Natural History, University of Helsinki, Finland.
[5]AMS Dating Laboratory, University of Århus, Denmark.
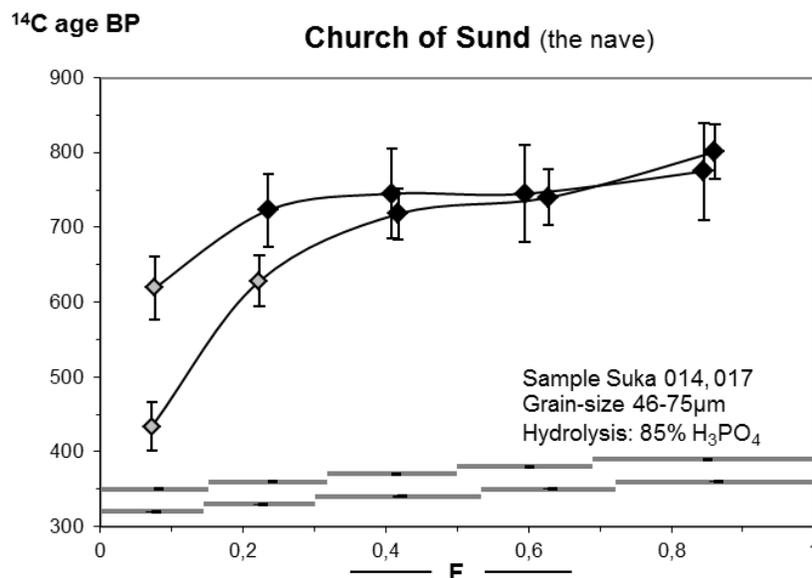
Figure 1 ^{14}C profiles from fire-damaged mortar samples produced by sequential hydrolysis with 85% H_3PO_4 (modified from Ringbom et al. 2005). The black dots denote the data used for calibrating the age in Table 1. CO_2 fraction sizes are presented along the abscissa as a function of the dissolution progress variable F ($0 \rightarrow 1$) in the order they are produced in CO_2 effervescence. F = 1 corresponds to (near total-total) dissolution overnight. ^{14}C profiles in this article will be presented in this way.

studying the mineralogy and the behavior of stable carbon and oxygen isotopes. The samples have earlier been dated, so a comparison with the preheating state can be made. The following Medieval churches and construction units within them will be considered (Table 1).

Table 1 Fire-damaged Medieval churches with the units we have tried to date as well as historically documented major fires are given. In case the ^{14}C distributions (column 4) are bimodal, only the first half is listed together with the probability. The second half for Turku cathedral can be rejected on stratigraphic grounds (based on plan views in Gardberg et al. 2000 and references therein). For Kumlinge, the second probability peak (31.4%, 2σ; Figure 6) cannot be rejected.

	Expected age (AD)	Ref.[a]	Our ^{14}C dating (2σ)	Documented major fire (AD)
Sund				
The nave	13th century	1	1240–1295	1678, 1921
Turku cathedral				
Sacristy 1	before 1291	2	1270–1300 (84.8%)	1318, 1656, 1681
Pentagonal choir	1300–	2	1310–1360 (50.7%)	1318, 1656, 1688, 1827
All Saints Chapel	ready 1471	2	1440–1485	1656, 1688, 1827
Kumlinge				
Nave, east gable	before 1484	3	1310–1360 (64.0%)	1714–1721
Nave, west gable	after east gable	3	1405–1435	no record
Föglö				
Nave, west gable	14th–15th centuries	3	possibly 14th century	1714–1721
Tower	after nave	3	1415–1445 (?)	1714–1721

[a]References: 1. Ringbom et al. (2005); 2. Gardberg et al. (2000); 3. Ringbom et al. (2011).

The goal of the study is thus to be able to identify fire-damage effects in a mortar even if it is not obvious at the sampling site. In this way, misinterpretation of the actual age of the structure can be avoided. We will also try to isolate post-fire carbonates from pre-fire carbonate so that we can get estimates of both the age of the building and later fierce fire events. The origin of the carbon will also be discussed: is it from the atmosphere or from burning wood?

FIRE DAMAGE

The cathedral in Turku, SW Finland, has burnt numerous times, the most recent fire being the great city fire in 1827. The structurally oldest part of the church, the first sacristy, may be the place where the first bishop, Magnus I, was elected in 1291. The church was inaugurated as cathedral in 1300 and destroyed by the Novgorodians in 1318 (e.g. Gardberg et al. 2000). All organic materials were burned as well as all documents in both the cathedral and in the bishops' residence castle in Kuusisto 15 km to the west. Fire damage is usually best identified in the actual ^{14}C profiles. It is, however, relatively common to have problems with the interpretation of the profiles because the dating method is expensive: one may have several contaminants and want to date as many samples as possible at the expense of the number of CO_2 fractions per sample. We have tried to overcome the dilemma by using some less-expensive methods, and studied the mineralogy and chemistry of the samples and the stable isotopes of the CO_2 fractions to see if there are any method that can provide helpful information for the interpretation of the age profiles.

Mineralogy

When mortar is dated, it is the binder carbonate mineral calcite that is the carbon source. The mineral is fairly heat-resistant. When the same mineral is burned in limestone to produce quicklime, temperatures over 900 °C have to be maintained for several days. Pure, single-crystal calcite or Iceland spar starts decomposing at 750 °C and the last Bragg peaks for calcite disappear at 800 °C (Ruiz-Agudo et al. 2008). "In the presence of water vapor at 1kbar, calcite begins to melt at 740°C. In the system $CaO+CO_2+H_2O$ at this pressure univariant equilibria $CaO+calcite+Ca(OH)_2+liquid$ and $calcite+Ca(OH)_2+liquid+vapor$ occur at 683°C and 675°C respectively" (Wyllie and Tuttle 1960). Christidis and Triantafyllou (2007 and references therein) report the beginning of the breakdown at 640 °C for Greek limestone and marbles. When there is dolomite, $CaMg(CO_3)_2$, present it must first be thermally dissociated:

$$CaMg(CO_3)_2 \rightarrow CaCO_3 + MgO + CO_2$$

The process starts at 687 °C, culminates at 773 °C, and ends at 781 °C. It is followed by breakdown of the calcite component:

$$CaCO_3 \rightarrow CaO + CO_2$$
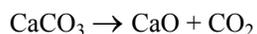
The breakdown starts at 781 °C, culminates at 834 °C, and ends at 916 °C (Gunasekaran and Anbalagan 2007 and references therein). Therefore, high decomposition temperatures are needed in limestone burning. Mortar calcite is, however, only poorly crystalline and it is rich in chemical impurities. Lower decomposition temperatures can thus be expected. Heating the samples to 650 °C already releases a considerable percentage of the carbon. The marble-based mortars from Turku cathedral: TTK 005 and 006 lost 20% and 18%, respectively, from their 76–150 µm grain-size fractions. This is nearly half of the theoretical maximum 44%. We studied the thermal breakdown using infrared spectroscopy (IR) and found that at 650 °C the remaining carbonate is not entirely calcite but a large part of it is transformed to vaterite (µ $CaCO_3$). At 750 °C, the CO_2 loss can be considered

nearly complete: 43% and 37% corresponding to 11.7% and 10.1% carbon. In Table 2, the carbon yields in acid hydrolysis from the 46–75 μm fractions were 10.2% and 10.3%.

Heating increases the solubility of the non-carbonate filler minerals, at least for the common silicates quartz and feldspars. Increased solubility of the silicates should cause raised hydraulic indices (HI), which are used to distinguish between lime mortar and concrete:

$$HI = (SiO_2 + FeO + Al_2O_3)/(CaO + MgO)$$

We tested the HI index change with 6 samples from Turku cathedral (Figure 2). The 151–300 μm grain-size fractions of the samples were each split into 2 aliquots. One was analyzed as such and the other was first heated for 2 hr at 650 °C and then analyzed after 1 week. Analyses were made with optical emission spectrometry (OES) at Åbo Akademi University. Some 300 mg of sample powder was leached in 10% HCl for 1 hr, and the solutions were analyzed together with a standard HCl solution containing the elements of interest. The error bars are estimated to be twice as large as for the standard solutions because of the disturbingly high calcium concentrations in the sample solutions (for Ca ±10% and for the other elements ±5%).
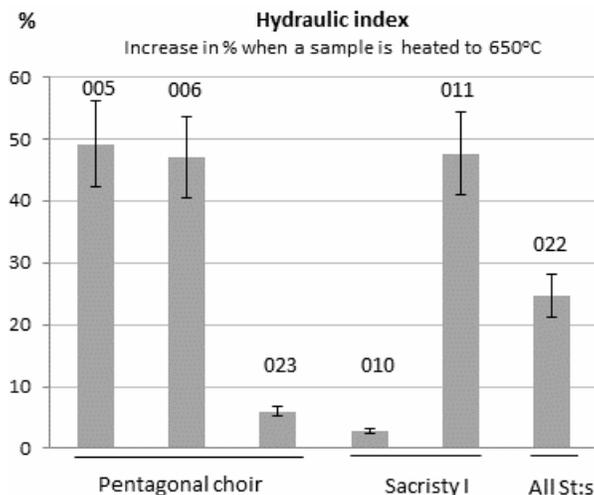

Figure 2 Test of solubility in standard HI determination. Percent increase of the HI of a sample aliquot after heating it to 650 °C compared with an unheated aliquot of the same sample powder.

The samples show considerable variation, and there is a trend that the fire-damaged samples are less affected by the heating. The All Saints Choir (sample 022) did burn in 1827 but still shows a 25% increase in HI. In the pentagonal choir, samples 005 and 006 show a large increase, but not sample 23 and the sacristy sample 10 is nearly intact while sample 011 is strongly affected. We have not studied the cause of the increased solubility of the silicates, but we consider the following possibilities: 1) burning the filler together with the carbonates is reminiscent of making concrete; 2) quartz grains are easily fractured when heated and fracturing increases the reaction surface.

Table 2 Data from hydrolysis with 85% H_3PO_4 and ^{14}C, $\delta^{13}C$, and $\delta^{18}O$ measurements.

Sample, grain-size fraction, & total carbon yield 85% H_3PO_4	CO_2 fraction (%)	Reaction time[a] (s)	Reaction temp.[b] (°C)	^{14}C age (yr BP)	$\delta^{13}C$ (‰)	$\delta^{18}O$ (‰)	Lab nr[c]
Church of Sund							
Suka 014 The Nave	0–14	16	0	496 ± 32	–22.3	–22.0	AAR-7563-1
46–75µm, 5.9%	15–30	65	0	683 ± 33	–11.7	–19.7	AAR-7563-2
	31–53	485	0	781 ± 33	–10.8	–17.8	AAR-7563-3
	54–72	1265	0	777 ± 36	–13.1	–19.8	AAR-7563-4
	73–100	overnight	ambient T	819 ± 33	–13.9	–19.5	AAR-7563-5
Suka 017 The Nave							
46–75µm, 5.9%	0–15	38	0	619 ± 42	–24.7	–22.5	AAR-7564-1
	16–32	90	0	723 ± 49	–15.1	–18.4	AAR-7564-2
	33–50	696	0	745 ± 60	–18.8	–20.2	AAR-7564-3
	51–69	2064	0	745 ± 65	–20.2	–20.9	AAR-7564-4
	70–100	overnight	ambient T	775 ± 65	–22.5	–20.6	AAR-7564-5
Turku Cathedral							
TTK 005-1 Pentagonal choir	0–5.3	10	0	552 ± 38	–21.7	–18.6	AAR-11016-1.1
46–75µm, 10.5%	5.4–18	50	0	643 ± 34	–9.8	–16.5	AAR-11016-1.2
	19–51	458	increasing	1048 ± 34	–10.8	–18.0	AAR-11016-1.3
	52–84	794	increasing	835 ± 35	–11.6	–20.8	AAR-11016-1.4
	85–100	overnight	ambient T	2241 ± 39	–10.1	–19.3	AAR-11016-1.5
TTK 005-3 Pentagonal choir							
46–75µm, 12%	0–7.8	3	ambient T		–23.6	–24.9	
Heated to 600 °C (2 hr)	7.9–23	16	ambient T		–11.2	–20.2	
	24–40	110	ambient T		–10.9	–18.0	
	41–80	1260	ambient T		–11.7	–20.7	
	81–100	11,300	ambient T		–11.0	–18.6	
TTK 005-4 Pentagonal choir							
46–75µm, 11.5%	0–3.5	2	ambient T		–25.0	–24.3	
Heated to 600 °C and 650 °C	3.6–19	10	ambient T		–12.7	–20.5	
(2 hr + 2 hr)	20–33	37	ambient T		–11.4	–17.9	
	34–46	130	ambient T		–11.7	–19.1	
	47–76	665	ambient T		–12.1	–20.5	
	77–93	1740	ambient T		–11.6	–19.7	
	94–99	7620	ambient T		–9.1	–17.2	
TTK 006 Pentagonal choir							
46–75µm, 10.3%	0–5.1	17	0	587 ± 35	–22.4	–19.6	AAR-11094-1
	5.2–19	97	0	720 ± 35	–8.9	–17.0	AAR-11094-2
	20–45	337	ambient T	1494 ± 33	–10.8	–18.4	AAR-11094-3
TTK 009 Sacristy I							
46–75µm, 3.5%	0–6	27	0	546 ± 26	–24.4		OxA-X-2209-7
	7–23	98	0	614 ± 25	–11.3		OxA-X-2210-47
	24–42	750	increasing	628 ± 25	–9.1		OxA-X-2210-48
TTK 009B.1 Sacristy I							
46–75µm, 7.4%	0–9.4	34	0	583 ± 25	–22.5		OxA-X-2226-30
	9.5–20	98	0	659 ± 25	–10.2		OxA-X-2226-31
	21–42	738	increasing	693 ± 23	–9.1		OxA-X-2227-50
	43–71	1450	increasing	670 ± 22	–10.4		OxA-X-2227-51
	72–100	68,400	ambient T	717 ± 24	–11.0		OxA-X-2227-51
TTK 009B.2 Sacristy I							
46–75µm, 9.3%	0–2.1	2	ambient T		–31.5	–26.3	
Heated to 600 °C (4 hr)	2.2–29	32	ambient T		–12.5	–22.2	
	30–44	49	ambient T		–10.8	–21.0	

Table 2 Data from hydrolysis with 85% H_3PO_4 and ^{14}C, $\delta^{13}C$, and $\delta^{18}O$ measurements. *(Continued)*

Sample, grain-size fraction, & total carbon yield 85% H_3PO_4	CO_2 fraction (%)	Reaction time[a] (s)	Reaction temp.[b] (°C)	^{14}C age (yr BP)	$\delta^{13}C$ (‰)	$\delta^{18}O$ (‰)	Lab nr[c]
	45–57	95	ambient T		–10.8	–21.5	
	58–92	600	ambient T		–11.3	–21.9	
	93–100	14,400	ambient T		–11.7	–21.6	
TTK 010 Sacristy I							
46–75µm, 3.6%	0–5.9	29	0	451 ± 27	–26.9		OxA-X-2209-8
	6–21	90	0	574 ± 25	–14.6		OxA-X-2210-49
	22–38	870	increasing	636 ± 25	–11.8		OxA-X-2210-50
TTK 010B Sacristy I							
46–75µm, 8.5%	0–9.8	39	0	541 ± 25	–22.6		OxA-X-2226-32
	9.9–22	120	0	612 ± 24	–9.7		OxA-X-2226-33
	23–40	637	increasing	674 ± 22	–7.7		OxA-X-2227-53
	41–70	1415	increasing	711 ± 22	–9.1		OxA-X-2227-54
	71–100	19,800	ambient T	643 ± 22	–9.3		OxA-X-2227-55
TTK 011 Sacristy I							
46–75µm, 9.9%	0–6.8	7	0	573 ± 35	–23.0	–22.4	AAR-11017-1
	6.9–24	53	0	599 ± 35	–9.0	–19.8	AAR-11017-2
	25–57	383	increasing	612 ± 38	–7.4	–21.1	AAR-11017-3
	58–90	815	increasing	615 ± 55	–8.6	–22.7	AAR-11017-4
	91–100	overnight	ambient T	793 ± 42	–9.7	–22.3	AAR-11017-5
TTK 021 All Saints choir							
76–150µm, 4.6%	0–6	27	0	250 ± 25	–25.7		OxA-X-2210-51
	7–16	92	0	379 ± 25	–10.0		OxA-X-2210-52
	17–36	345	0	417 ± 24	–10.0		OxA-X-2210-53
	37–57	1020	increasing	388 ± 25	–12.5		OxA-X-2210-54
TTK 022 All Saints choir							
46–75µm, 7.6%	0–11	18	0	254 ± 35	–24.4	–20.4	AAR-11018-1
	12–36	80	0	413 ± 32	–6.9	–17.4	AAR-11018-2
	37–61	330	increasing	447 ± 30	–9.0	–18.4	AAR-11018-3
	62–85	444	increasing	392 ± 36	–9.6	–19.5	AAR-11018-4
	86–100	overnight	ambient T	598 ± 37	–11.0	–20.4	AAR-11018-5
TTK 023 Pentagonal choir							
46–75µm, 10.2%	0–5.3	n.r.	0	559 ± 26	–22.8	–10.2	AAR-11498-1
	5.4–17	n.r.	0	704 ± 41	–8.9	–7.7	AAR-11498-2
Church of Kumlinge							
Kumka 001 West gable	0–17	n.r.	0	428 ± 24	–15.1	–17.3	AAR-11852-1
46–75µm, 2.8%	18–36	n.r.	0	495 ± 27	–4.2	–13.2	AAR-11852-2
	37–61	n.r.	increasing	528 ± 28	–9.4	–16.1	AAR-11852-3
Kumka 002 West gable							
46–75µm, 7.4%	0–19	n.r.	0	535 ± 29	–15.2	–18.1	AAR-11853-1
	20–43	n.r.	increasing	516 ± 29	–6.6	–14.7	AAR-11853-2
	44–69	n.r.	increasing	489 ± 26	–10.8	–17.3	AAR-11853-3
Kumka 003 West gable							
46–75µm, 5.8%	0–12	n.r.	0	512 ± 36	–16.9	–15.8	AAR-12319-1
	13–35	n.r.	increasing	491 ± 42	–5.6	–12.0	AAR-12319-2
	36–53	n.r.	increasing	583 ± 40	–9.6	–13.6	AAR-12319-3
Kumka 004 East gable							
46–75µm, 7.5%	0–15	n.r.	0	251 ± 27	–11.4	–16.0	AAR-11854-1
	16–38	n.r.	increasing	634 ± 49	–8.2	–15.2	AAR-11854-2
	39–63	n.r.	increasing	607 ± 34	–11.7	–18.1	AAR-11854-3

Table 2 Data from hydrolysis with 85% H_3PO_4 and $[14]C$, $\delta^{13}C$, and $\delta^{18}O$ measurements. *(Continued)*

Sample, grain-size fraction, & total carbon yield 85% H_3PO_4	CO_2 fraction (%)	Reaction time[a] (s)	Reaction temp.[b] (°C)	$[14]C$ age (yr BP)	$\delta^{13}C$ (‰)	$\delta^{18}O$ (‰)	Lab nr[c]
	64–87	n.r.	increasing	603 ± 31	–11.9	–18.3	AAR-11854-4
	88–100	n.r.	ambient T	806 ± 27	–12.3	–18.2	AAR-11854-5
Kumka 005 East gable							
46–75μm, 6.0%	0–11	n.r.	0	294 ± 48	–15.5	–18.2	AAR-12320-1
	12–35	n.r.	increasing	420 ± 34	–4.9	–16.0	AAR-12320-2
	36–58	n.r.	increasing	550 ± 35	–9.2	–17.9	AAR-12320-3
	59–80	n.r.	increasing	549 ± 25	–10.6	–19.3	AAR-12320-4
	81–100	n.r.	ambient T	678 ± 25	–11.3	–19.0	AAR-12320-5
Church of Föglö							
Foka 001 Nave	0–13	n.r.	0	393 ± 34	–22.0	–20.5	AAR-11855-1
46–75μm, 8.4%	14–33	n.r.	increasing	571 ± 32	–11.0	–17.9	AAR-11855-2
	34–57	n.r.	increasing	560 ± 39	–12.3	–19.2	AAR-11855-3
Foka 003 Nave	0–11	n.r.	0	610 ± 31	–20.7	–20.7	AAR-11857-1
46–75μm, 8.8%	12–34	n.r.	increasing	714 ± 28	–8.8	–18.6	AAR-11857-2
	35–55	n.r.	increasing	1085 ± 46	–9.9	–19.3	AAR-11857-3
Foka 004 Tower	0–9.1	n.r.	0	338 ± 41	–23.4	–14.9	AAR-12323-1
46–75μm, 6.5%	9.2–29	n.r.	0	466 ± 30	–13.5	–15.4	AAR-12323-2
	30–47	n.r.	increasing	636 ± 33	–13.7	–15.6	AAR-12323-3
Foka 006 Tower	0–9.1	n.r.	0	475 ± 35	–26.1	–19.3	AAR-12324-1
46–75μm, 8.0%	9.2–29	n.r.	0	589 ± 35	–11.4	–17.5	AAR-12324-2
	30–47	n.r.	increasing	694 ± 44	–10.7	–17.6	AAR-12324-3
Foka 007 Tower	0–9.3	n.r.	0	323 ± 35	–20.4	–19.9	AAR-12325-1
46–75μm, 7.6%	9.4–30	n.r.	0	493 ± 36	–6.9	–17.6	AAR-12325-2
	31–49	n.r.	increasing	481 ± 34	–9.2	–18.7	AAR-12325-3
Foka 008 Tower	0–9.7	n.r.	0	356 ± 47	–22.7	–18.16	AAR-12326-1
46–75μm, 6.7%	9.8–32	n.r.	0	495 ± 31	–14.9	–16.6	AAR-12326-2
	33–47	n.r.	increasing	606 ± 22	–15.79	–17.89	AAR-12326-3

[a] n.r. = not registered.

[b] ambient T = ambient lab temperature.

[c] AAR = Aarhus AMS lab; AA = NSF-Arizona AMS lab; OxA-X = Oxford ORAU; No number = Finnish Museum of Natural History.

[14]C Profiles

We wanted to test mortar dating because we had promising results from the fire-damaged church of Sund (Figure 1). We also wanted to learn more about mortars made of extremely pure marble. We have previously dated mortars made from Estremoz marble in Portugal (Langley et al. 2011) with conclusive results from ordinary-looking profiles. The cathedral in Turku, SW Finland, is situated in a basement rock area where there are no limestones available for lime production, but only marble. The church has burnt numerous times. In this article, we will discuss the samples from the first sacristy, from a sheltered place under the pentagonal choir, and from the All Saints chapel that has suffered from repeated fires (see results in Table 2). The sample sites and additional ^{14}C results from the cathedral are published in Lindroos et al. (2011).

The original wall of the pentagonal choir has been preserved in a tomb under the floor level. Here we found mortar that seemed unaffected by fire. The samples (TTK 005, 006, and 023) yielded typical ^{14}C profiles with strong dead-carbon contamination (Figure 3). The dead carbon comes from the marble. There are marble grains that are easily discernible in cathodo-luminescence (CL) and it is most likely that the mortar has been produced by burning marble from the Medieval quarry in Pargas about 20 km to the south (see Boström 1986). The date of AD 1310–1360 (Table 1), based on a combination of the first fractions in the profiles, does not resolve whether the mortar is original or a repair after the destruction 1318.
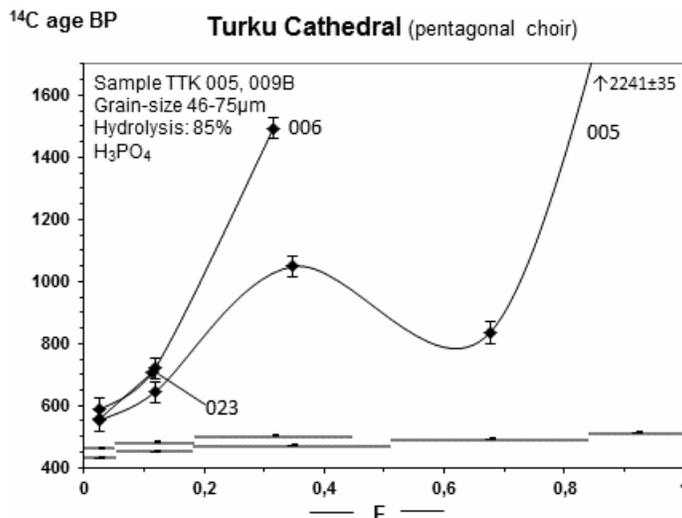
Figure 3 ^{14}C profiles from a tomb under the pentagonal choir in Turku cathedral

^{14}C profiles from the burned first sacristy are completely different (Figure 4). Samples (009, 009B, 010, 010B, and 011; Table 2) are from a sooty wall above ground level in the interior. The sacristy was the only part of the church that survived the great city fire in 1827, so this fire damage is older.

We have interpreted the results as follows: Sample 011 yields a very well-behaved ^{14}C profile for dating. It is flat all the way to the fifth CO_2 fraction, meaning that it is devoid of contaminating filler carbonate of geological origin, which would create a bump in the profile similar to the one in Figure 2. ^{14}C ages of the first 4 fractions overlap clearly and yield the combined age 596 ± 19 BP, or cal AD 1300–1370 (73.1%) or 1380–1410 (22.3%) at 95.4% probability. Profiles 009B and 010B have been interpreted so that the overlapping ^{14}C ages for the CO_2 fractions 009B.2,3,4,5 and 010B.3,4,5 give the binder carbonate age 681 ± 9 BP (cal AD 1270–1300; 84.8% at 95.4% confidence level) and the first fractions are affected by younger carbonates after one or several fires. BP ages have been calibrated using OxCal v 3.10 (Bronk Ramsey 1995, 2001) and the IntCal04 calibration curve (Reimer et al. 2004).

Samples 021 (4 CO_2 fractions) and 022 (5 CO_2 fractions) from the All Saints Chapel, finished in 1471, were taken for reference. We wanted to have samples that were certainly damaged by the fire in 1827 and also in the fires of 1656 and 1681. They were also most likely made from similar marble as the other mortars. The fires in 1827 and 1681 meant total destruction except for the mortared walls; even the church bells melted. Figure 5 shows the results for 2 mortars from the chapel. The profile of TTK 022 is similar to the ones from the burned church of Sund (Figure 1) and TTK 009B,
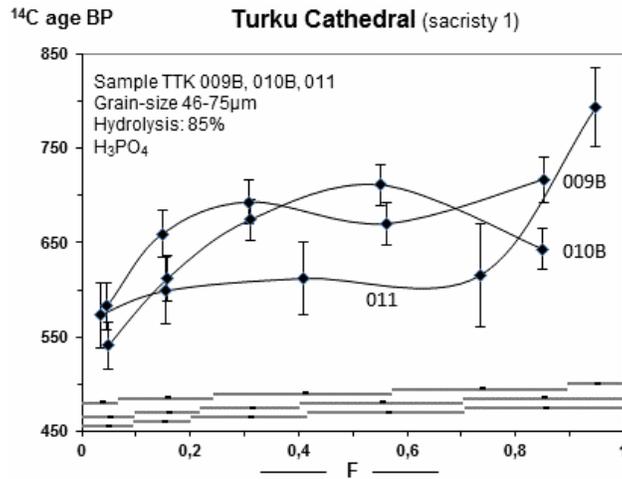
Figure 4 ^{14}C profiles from the oldest part of the church. Is the binder age defined by the first CO_2 fractions, which all overlap in age or does sample 011 represent another type of mortar, maybe a repair after the fire in 1318?

010B (Figure 4). The mid-fractions give the right archaeological age and together they comprise 74% of the available carbon. The first fractions of both profiles yield an age of 250 BP. This age corresponds fairly well with the great fire in 1681 considering that the fractions certainly also contain some original binder CO_2 from 1466–1471.
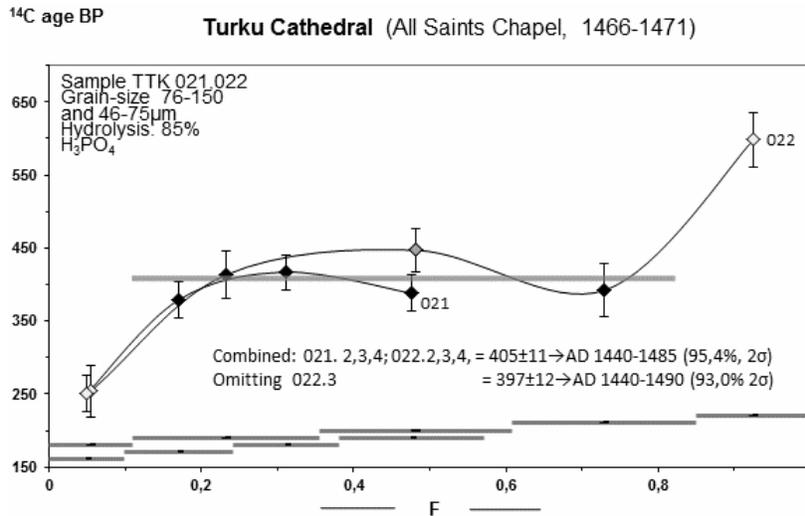
Figure 5 ^{14}C profiles of fire-damaged mortars. The mid-fractions represent the known archaeological age of 1466–1471, while the first carbonate to dissolve is younger and the last carbonate is older. Two calibrations are made: A) for all fractions 2, 3, and 4 (black dots and gray line); B) leaving out 023.3 (gray dot) because of possible marble contamination.

The Medieval church of Kumlinge Island is located 85 km W-SW from Turku in the Åland Archipelago between Finland and Sweden. It was first mentioned in written sources in 1484 (Ringbom et al. 2011 and references therein). The church is built from mortared field stones. It is situated on the

same metamorphic basement rocks as Turku cathedral, but there are no marble deposits in the vicinity. We have not studied the provenance of the lime, but we assume that it was made on the nearby main island by burning Ordovician limestone from blocks lying around in the terrain. The eastern and western gables of the church are clearly different: in the attic, where we took the samples one can see that the eastern gable is fire damaged with cracking granite blocks and only scarce mortar left between the stones, while the in western gable the stone blocks look unharmed and there is plenty of mortar between them. Figure 6 presents ^{14}C profiles from the burnt east gable and Figure 7 from the west gable.
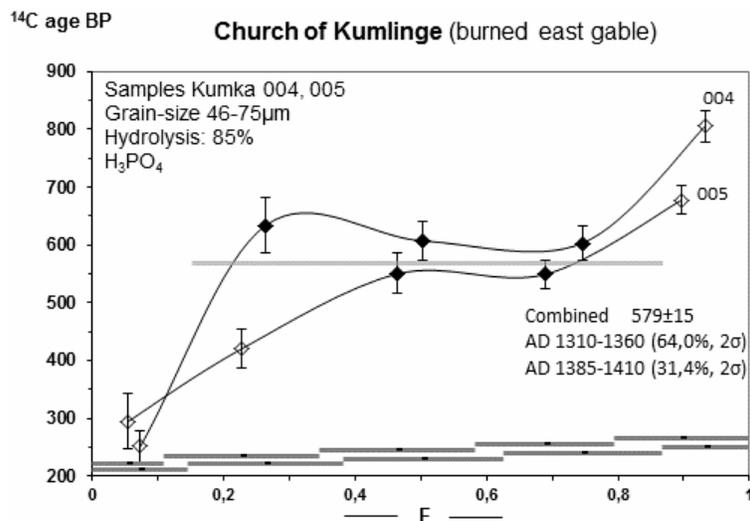
Figure 6 ^{14}C profiles of fire-damaged mortars from the church of Kumlinge, SW Fin-
land. The combined calibration is for the data points with filled dots.

The church of Föglö Island is 34 km SW of Kumlinge on the same metamorphic basement. There are no marble deposits here either, so the situation is the same as in Kumlinge: the lime is probably made from Ordovician limestone on the main island. The chronology of the church is poorly known. It was burned during the Great Northern War (1714–1721) and rebuilt in the 1850s. The only original parts remaining are the westernmost parts of the nave and the adjoining tower. The Medieval altar was recovered against the original east wall of the chancel. It contained a silver reliquary from around 1400. Out of 57 Medieval coins found in the church, 17 belonged to the 14th century; several of them were found close to the altar. Two samples from the west gable of the nave gave inconclusive ^{14}C profiles (Figure 8).

^{14}C profiles from the tower are also ambiguous, partly because they have only 3 CO_2 fractions per profile (Figure 9) and mainly because there is a lot of contamination making the profiles steeply inclined. We do not yet have enough unambiguous data for dating the tower, so we can only present tentative interpretations. Two different interpretations are suggested in Figure 9: 1) there are no recrystallizations and the cluster of 3 data points for the 3 first fractions at ~338 BP give the ^{14}C age of the tower (e.g. Heinemeier et al. 2010); 2) there are rapidly dissolving young recrystallizations because the profiles are linear and steeply inclined or bend the other way compared with TTK 005 and 006 (Figure 3) and Foka 003 (Figure 8). The actual age of the tower is Medieval and is vaguely defined by the plateau-like cluster of gray dots.
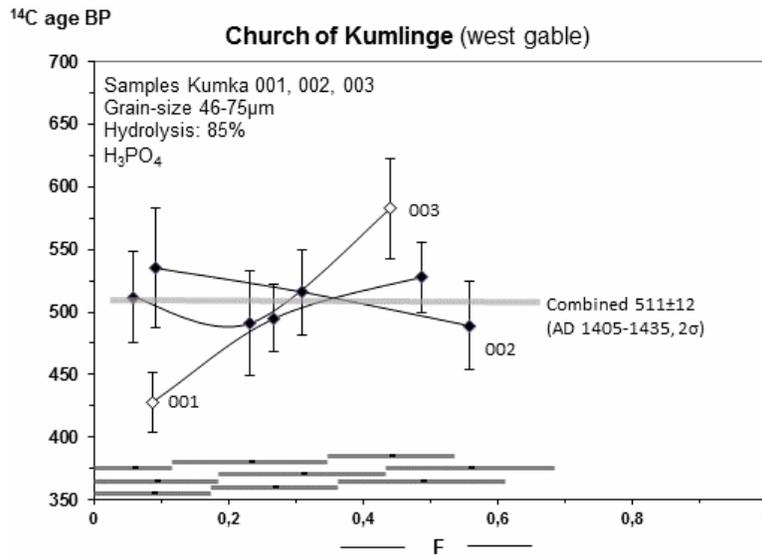
Figure 7 ^{14}C profiles from the west gable of the church of Kumlinge. There are no indications of fire damage at the sampling site. Only profile 001 has similarities with profiles from fire-damaged mortars. There are only 3 CO$_2$ fractions per profile for economic reasons. The combined calibration is for the data points with filled dots.
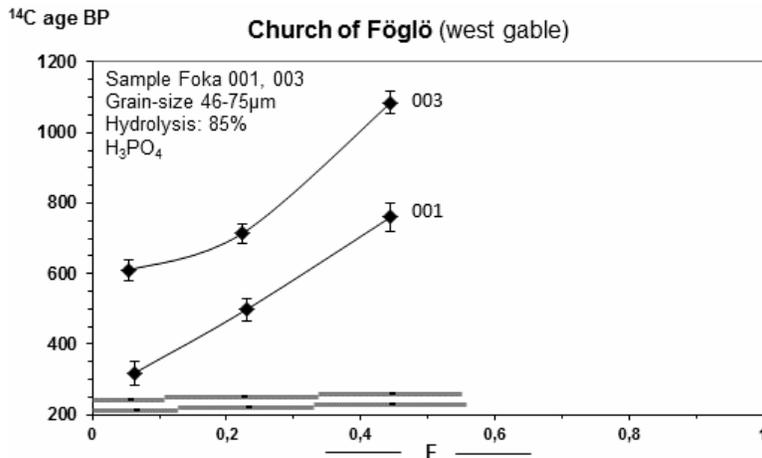

Figure 8 ^{14}C profiles from the west gable of the nave in the church of Föglö. Profile 001 is difficult to interpret, and we have not tried to use it for dating the church. Profile 003 may indicate a 14th century age if interpreted the same way as profiles 005 and 006 in Figure 2.

Stable Isotopes

δ^{13}C values are measured as a routine in ^{14}C dating because the parameter is used for correcting the ^{14}C ages in response to chemical fractionation of the carbon isotopes. The measurement is done with IRMS on an aliquot of the same CO$_2$ gas that is graphitized for the AMS. The ^{18}O/^{16}O ratio of the CO$_2$ is also measured because it interferes with the molecular weight. We therefore have both the δ^{13}C and δ^{18}O values for a number of samples (Table 2). It should be noted that the values have been
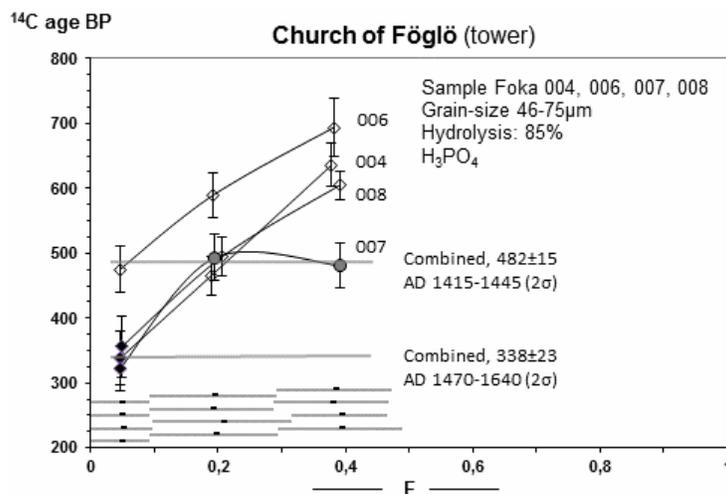
Figure 9 Four steeply inclined ^{14}C profiles from the tower of the church of Föglö indicating severe contamination. Two interpretations are indicated: 1) there is only limestone contamination and a young archaeological age can be read from the cluster of first fractions (black dots). 2) there is recarbonation after a fire (black dots) and the true age is defined by fractions 2 and 3 of sample 007 (gray dots) and possible the first fraction of sample 006.

produced using 85% H_3PO_4 and not in the standard way using dry acid. Note also that different reaction temperatures may have been used. Therefore, the reported $\delta^{18}O$ values are comparable only within this study and with values reported for mortars by the Århus lab (e.g. in Lindroos et al. 2007; Heinemeier et al. 2010; Ringbom et al. 2011). Usually, preparation for dating was done at 0 °C, for the first 2 CO_2 fractions; whereas later stable isotope measurements for the same sample aliquots were made on CO_2 produced at ambient lab temperatures. The fractionation factor σ_T for $\delta^{18}O$ is 1.01025 at 0 °C and 1.01025 at 25 °C (Friedman and O'Neil 1977). The effect of the temperature on the fractionation is negligible when total dissolution is performed and insignificant for the conclusions when partial dissolution is used because lower temperatures should yield lower δ values. (We have higher values for the sample aliquots prepared at 0 °C compared with the values we received after heating and then dissolution at ambient lab temperature.)

We noted earlier that it is common for fire-damaged mortars to react violently in acid hydrolysis and that their first CO_2 fractions have very negative $\delta^{13}C$ values. Values < –22‰ PDB should be considered abnormal because the $\delta^{13}C$ value of the atmospheric CO_2 source is around –7. There is a strong kinetic fractionation when alkaline mortar comes in contact with the air and mortar values are usually < –7, but the fractionation should not yield values < –21 (O'Neil and Barnes 1971; MacLeod et al. 1990; Van Strydonck et al. 1989). Lower values can only be obtained if additional fractionating reactions occur. In Figure 10, we plotted the stable isotope values of the first CO_2 fractions for each sample as a function of the dissolution progress parameter F. Because we were not sure that any of the samples are unaffected by fire, we included some samples from the Medieval church of Kökar (open dots) that have no known fires in its history. The church is situated 36 km south of Kumlinge on Precambrian gneisses with no marble nor limestone deposits.

There is an intrinsic trend in Figure 10 that is not obvious but should be considered: CO_2 fractions with small F values are more negative than others because (A) there is a strong kinetic fractionation in the hydrolysis reaction the first seconds lowering the values and (B) there might be lime lumps
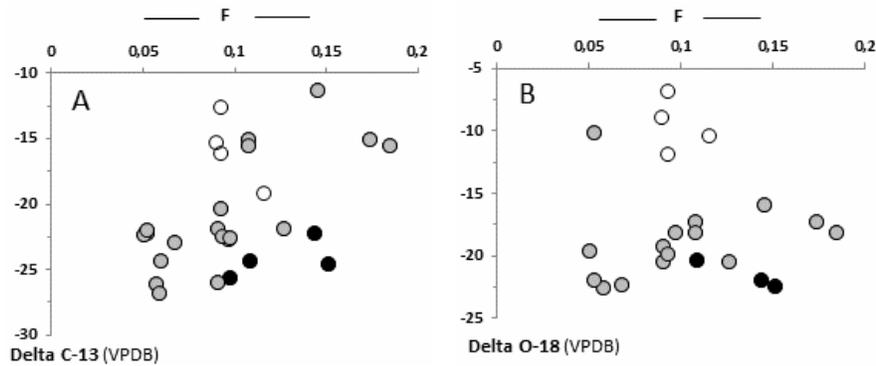
Figure 10 Stable isotope values for the first CO_2 fractions of samples discussed earlier. Samples with known fire damage in black from Sund church and the All Saints choir of Turku cathedral. Samples with suspected fire damage from Föglö, Kumlinge, and sacristy I and the pentagonal choir of Turku cathedral are marked with gray dots. Samples denoted with open dots are reference samples from the church of Kökar with no known fires in its history (data from Ringbom et al. 2011).

raising the values if the reactions time is extended and a large fraction is collected. There is still a trend that fire-damaged samples have very negative δ values. The Sund and All Saints Chapel samples have F values >0.1, but they are still among the most negative ones. The Kökar samples have similar or lower F values, but clearly higher δ values. The very distinct difference in $\delta^{18}O$ between the Kökar samples and the rest of the samples, excluding TTK 023 (the pentagonal choir), is difficult to explain since the oxygen isotopes are also affected by the slaking water and water added with the aggregate.

We tested 2 samples to better understand the chemical activity of the stable isotopes. The remaining 46–75 µm grain-size fraction of sample TTK 005 from the pentagonal choir and the residue of sample TTK 009B (sacristy I) of Turku cathedral were heated, first at 600 °C and then at 650 °C (after drying them at 105 °C for 24 hr and heating them at 550 °C for 4 hr). TTK 005 we split into 2 aliquots and removed the other from the oven already after it had been heated at 600 °C. All aliquots were in the oven at 600 °C for 2 hr and the second aliquot of sample 005 and sample 009B additionally 2 hr at 650 °C. After the heating, we registered the weight loss and let the samples reside in the laboratory atmosphere over the weekend. After the weekend, we measured the weight gain and then performed acid hydrolysis on the grain-size fractions in the same manner as we do when we prepare samples for ^{14}C dating (e.g. Heinemeier et al. 2010). This time, we measured the stable isotopes only. The change in weight during the procedure is presented in Figure 11.

We can see again that sample 009B with a history of earlier fire damages is less affected than sample 005. The regaining of carbon during the weekend remained incomplete. The aliquot that was only heated at 600 °C showed a 0.9% lighter weight after the weekend, which is strange. It is probably only a measurement problem due to rapid moisture uptake.

The stable isotopes trend towards lighter signatures in sample 005 after heating (Figure 12). When we consider the whole carbon inventory (calculated as the weighted average of the values for the individual CO_2 fractions), there is a slight 0.9‰ decrease in $\delta^{13}C$ and a 1.1‰ decrease in $\delta^{18}O$ when samples were heated to 600 °C, but then a minor increase when the powders were further heated to 650 °C. This may be due to the short and uncompleted recovery during only 1 weekend (Figure 11). Sample 009B has no $\delta^{18}O$ data in the original ^{14}C report, so we could only compare the $\delta^{13}C$ values. There is no change in the values (Table 2) due to the heating even if the regaining is incomplete.

% weight loss relative the weight at 550 deg. C
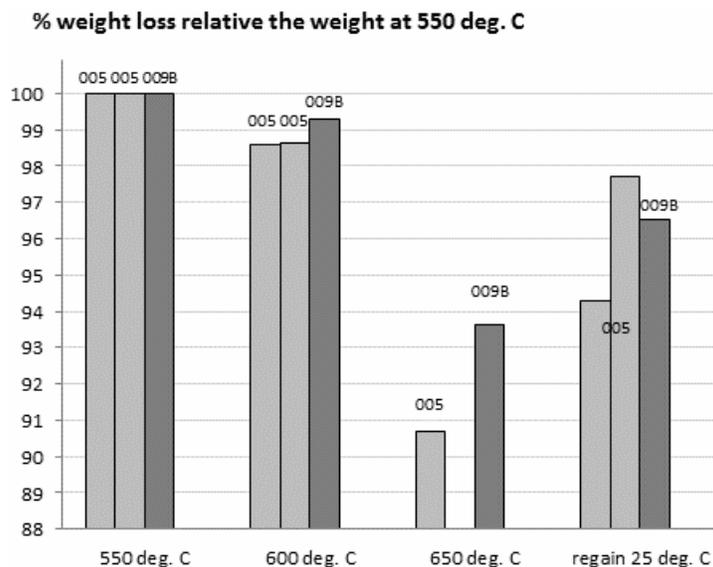
Figure 11 Weight loss at heating and weight gain after cooling down for a sample that show no signs of fire damage (005) and another that suffered fire damage earlier in its history (009B). Two aliquots of sample 005 were heated, but the other was removed from the oven after heating at 600 °C. We used the weight after 550 °C as reference so that the combustion of organic matter would no longer interfere with the weights.
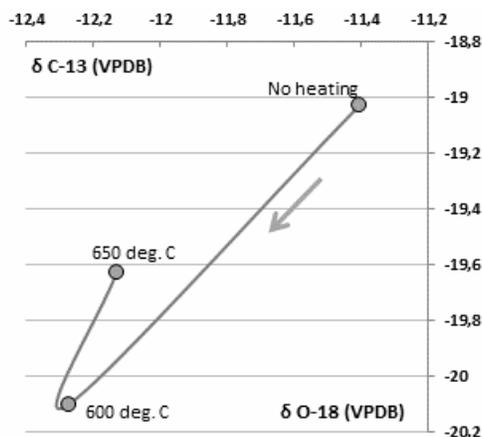

Figure 12 $\delta^{13}C$ and $\delta^{18}O$ trends when the powder of sample TTK 005 was heated at 600 °C and 650 °C, respectively.

The individual CO_2 fractions display larger variability (Figures 13 and 14). There is a general trend that the heating has produced readily soluble carbonates enriched in ^{12}C and especially ^{16}O, while the slowly dissolving ones are little affected. There seems, though, to be an enrichment of heavy isotopes in the last carbonates to dissolve when the mortar has not been heated before in a fire (Figure 13A).
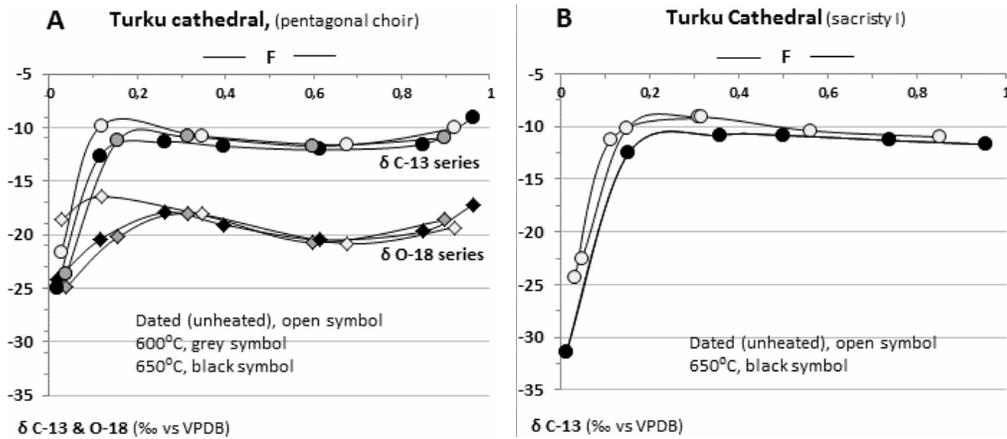
Figure 13 Stable carbon and oxygen isotope fractionation induced by heating sample aliquots. Open markers denote unheated aliquots, gray markers heating at 600 °C, and black markers heating at 650 °C. The mortar in (A) has probably not been heated before, while the mortar in (B) has been exposed to historical fires (Table 1).

In Figure 14, we can see that the heating of sample TTK 005 (data from Figure 13A) has affected fractions 1 and 2 very clearly. Thereafter, fractions 3 and 4 are similar for heated and unheated aliquots and then fraction 5 deviates again.
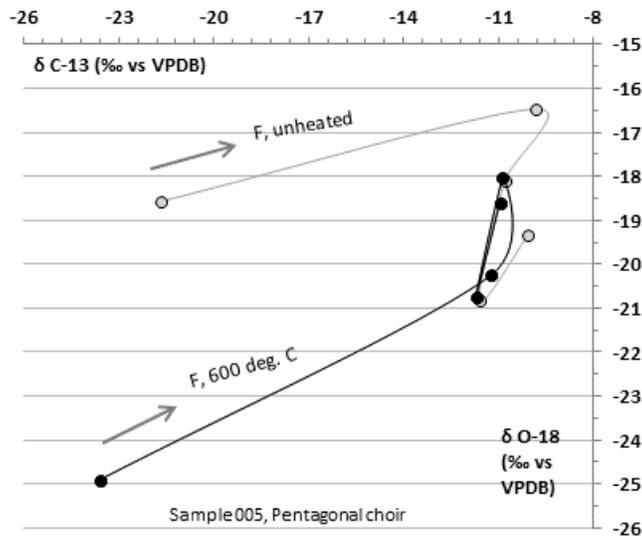

Figure 14 $\delta^{13}C$ vs. $\delta^{18}O$ for 5 CO_2 fractions for an unheated sample aliquot and a heated aliquot (600 °C).

DISCUSSION

Our preliminary results indicate that fire damage affects ^{14}C dating of mortars when temperatures reach ~600 °C. Increasing temperatures make the carbonates unstable and they begin interacting with other minerals in temperature-controlled equilibrium conditions. A substantial part of the calcite is transformed to vaterite, which is stable at least for months after the mortar has cooled down.

Thermal treatment increases the solubility of the mortars in phosphoric acid. The newly formed carbonates dissolve extremely rapidly, and it might be difficult to extract a CO_2 fraction <10% of the total CO_2 yield because it has to be done within seconds. Such small initial CO_2 fractions have ^{14}C from the fire event, and their ^{14}C age approaches the age of that event when the CO_2 fraction is minimized. Typically, a past fire event is identified from the ^{14}C profile because the first CO_2 fraction is younger than the subsequent ones. More precisely, the difference between the first and the second CO_2 fractions is larger than the difference between the second and the third fractions. Also, the silicate filler minerals show increased solubility after thermal treatment, and it might be worth studying more systematically how well the increased solubility correlates with the treatment temperature and if it can be used as an indicator of historical fire damage or rather the absence of fire damage.

Fire-damaged samples tend to have very light isotopic signatures for the stable isotopes of carbon and oxygen in initially extracted CO_2. It is not necessary to introduce CO_2 from burning wood to get the low values. They can be obtained in response to repeated kinetic fractionation when $Ca(OH)_2$ is produced in the heat and moisture of fires.

ACKNOWLEDGMENTS

REFERENCES

Boström R. 1986. The history of the stone and mineral industry in Finland. *Geological Survey of Finland, Bulletin* 336:273–98.

Bronk Ramsey C. 1995. Radiocarbon calibration and analysis of stratigraphy: the OxCal program. *Radiocarbon* 37(2):425–30.

Bronk Ramsey C. 2001. Development of the radiocarbon calibration program. *Radiocarbon* 43(2A):355–63.

Christidis GE, Triantafyllou G. 2007. Influence of particle size on the thermal decomposition of calcite. *Acta Crystallographica A* 63:265–66.

Friedman I, O'Neil JR. 1977. Compilation of stable isotope fractionation factors of geochemical interest. In: *Data of Geochemistry*. US Geological Survey, Professional Paper 440 KK, 6th edition.

Gardberg CJ, Heininen S, Welin PO. 2000. *Nationalhelgedomen Åbo Domkyrka 1300–2000*. Helsingfors: Tammi Förlag. 384 p. In Swedish with English summary.

Gunasekaran S, Anbalagan G. 2007. Thermal decomposition of natural dolomite. *Bulletin of Material Sciences* 30(4):339–44. Indian Academy of Sciences.

Hajdas I, Trumm J, Bonani G, Biechele C, Maurer M, Wacker L. 2012. Roman ruins as an experiment for radiocarbon dating of mortar. *Radiocarbon*, these proceedings.

Heinemeier J, Jungner H, Lindroos A, Ringbom Å, von Konow T, Rud N. 1997. AMS ^{14}C dating of lime mortar. *Nuclear Instruments and Methods in Physics Research B* 123:487–95.

Heinemeier J, Ringbom Å, Lindroos A, Sveinbjörnsdót-

tir ÁE. 2010. Successful AMS ^{14}C dating of non-hydraulic lime mortars from the medieval churches of the Åland Islands, Finland. *Radiocarbon* 52(1):171–204.

Hodgins GWL, Lindroos A, Ringbom Å, Heinemeier J, Brock F. 2011. [14]C dating of Roman mortars – preliminary tests using diluted hydrochloric acid injected in batches. In: Ringbom Å, Hohlfelder R, editors. *Commentationes Humanarum Litterarum, Societas Scientiarium Fennica*. Proceedings from Building Roma Aeterna Conference in Rome, 23–25 March 2008. p 209–13.

Langley MM, Maloney SJ, Ringbom Å, Heinemeier J, Lindroos A. 2011. A comparison of dating techniques at Torre de Palma, Portugal: mortars and ceramics. In: In: Ringbom Å, Hohlfelder R, editors. *Commentationes Humanarum Litterarum, Societas Scientiarium Fennica*. Proceedings from Building Roma Aeterna Conference in Rome, 23–25 March 2008. p 242–56.

Lindroos A, Heinemeier J, Ringbom Å, Braskén M, Sveinbjörnsdóttir ÁE. 2007. Mortar dating using AMS ^{14}C and sequential dissolution: examples from medieval, non-hydraulic lime mortars from the Åland Islands, SW Finland. *Radiocarbon* 49(1):47–67.

Lindroos A, Ringbom Å, Kaisti R, Heinemeier J, Hodgins G, Brock F. 2011. The oldest parts of Turku cathedral. C-14 chronology of fire damaged mortars. In: Hansson J, Ranta H, editors. *Archaeology and History of Churches in Baltic Region*. County Administrative Board of Gotland and Gotland University. p 108–21.

MacLeod G, Hall AJ, Fallick AE. 1990. An applied min-

eralogical investigation of concrete degradation in a major concrete road bridge. *Mineralogical Magazine* 54:637–44.

Nawrocka D, Czernik J, Goslar T. 2009. 14C dating of carbonate mortars from Polish and Israeli sites. *Radiocarbon* 51(2):857–66.

O'Neil JR, Barnes I. 1971. C13 and O18 compositions in some fresh-water carbonates associated with ultramafic rocks and serpentinites: western United States. *Geochimica et Cosmochimica Acta* 35(7):687–97.

Pesce G, Quarta G, Calcagnile L, D'Elia M, Cavaciocci P, Lastrico C, Guastella R. 2009. Radiocarbon dating of lumps from aerial lime mortars and plasters. *Radiocarbon* 51(2):867–72.

Reimer PJ, Baillie MGL, Bard E, Bayliss A, Beck JW, Bertrand CJH, Blackwell PG, Buck CE, Burr GS, Cutler KB, Damon PE, Edwards RL, Fairbanks RG, Friedrich M, Guilderson TP, Hogg AG, Hughen KA, Kromer B, McCormac G, Manning S, Bronk Ramsey C, Reimer RW, Remmele S, Southon JR, Stuiver M, Talamo S, Taylor FW, van der Plicht J, Weyhenmeyer CE. 2004. IntCal04 terrestrial radiocarbon age calibration, 0–26 cal kyr BP. *Radiocarbon* 46(3):1029–58.

Ringbom Å, Bartholin T, Klein P, Lindroos A, Sveinbjörnsdóttir ÀE, Heinemeier J. 2005. Naturvetenskaplig datering. In: Ringbom Å, Remmer C, editors. *Ålands Kyrkor, Volume III*. Sund och Vårdö: Ålands Landskapsstyrelse/museibyrå. 336 p. In Swedish with English summary.

Ringbom Å, Lindroos A, Heinemeier J, Gustavsson K. 2011. Dating stone churches in the outer Åland archipelago. In: Hansson J, Ranta H, editors. *Archaeology and History of Churches in Baltic Region*. County Administrative Board of Gotland and Gotland University. p 141–70.

Ruiz-Agudo E, Rodrígues-Navarro C, Luque A, Rodrígues-Navarro A, Huertas MO. 2008. A TEM and 2D-XRD study of the thermal decomposition of calcite. *Macla* [Revista de la Sociedad Española de Mineralogía] 9:223–4.

Tubbs LE, Kinder TN. 1990. The use of AMS for the dating of lime mortars. *Nuclear Instruments and Methods in Physics Research B* 52(3–4):438–41.

Van Strydonck M, Dupas M, Keppens E. 1989. Isotopic Fractionation of oxygen and carbon in lime mortar under natural environmental conditions. *Radiocarbon* 31(3):610–8.

Van Strydonck MJY, van der Borg K, de Jong AFM, Keppens E. 1992. Radiocarbon dating of lime fractions and organic material from buildings. *Radiocarbon* 34(3):873–9.

Wyllie PJ, Tuttle OF. 1960. The system CaO-CO$_2$-H$_2$O and the origin of carbonatites. *Journal of Petrology* 1: 1–46.